

# Nitric Oxide Modulates Fracture Healing

Ashish D. Diwan M.B.B.S, M.S.

Min X. Wang

Daniel Jang

Wei Zhu

George A. C. Murrell

First published: 18 February 2010

<https://doi.org/10.1359/jbmr.2000.15.2.342>

Cited by: 80

SECTIONS



PDF

TOOLS

SHARE

## Abstract

The role of the messenger molecule nitric oxide has not been evaluated in fracture healing. NO is synthesized by three kinds of nitric oxide synthase (NOS): inducible NOS (iNOS), endothelial (eNOS), and neuronal (bNOS). We evaluated the role of these enzymes in a rat femur fracture-healing model. There was no messenger RNA (mRNA) expression, immunoreactivity, or enzymatic activity for NOS in unfractured femoral cortex. After fracture, however, mRNA, protein, and enzymatic activity for iNOS were identified in the healing rat femoral fracture callus, with maximum activity on day 15. The mRNA expression for eNOS and bNOS was induced slightly later than for iNOS, consistent with a temporal increase in calcium-dependent NOS activity that gradually increased up to day 30. mRNA expression for the three NOS isoforms also was found in six of six human fracture callus samples. To study the effect of suppression of NO synthesis on fracture healing, an experimental group of rats was fed an NOS inhibitor, L-nitroso-arginine methyl ester (L-NAME), and the control group was fed its inactive enantiomer, D-nitroso-arginine methyl ester (D-NAME). An 18% ( $p \leq 0.01$ ) decrease in cross-sectional area and a 45% ( $p \leq 0.05$ ) decrease in failure load were observed in the NOS-inhibited group on day 24 after fracture. Furthermore, the effect of NO supplementation to fracture healing was studied by delivering NO to the fracture site using carboxybutyl chitosan NONOate locally. On day 17 after fracture, there was a 30% ( $p \leq 0.05$ ) increase in cross-sectional area in the NO-donor group compared with the NOS inhibition group. These results show for the first time that NO is expressed during fracture healing in rats and in humans, that suppression of NOS impairs fracture healing, and that supplementation of NO can reverse the inhibition of healing produced by NOS inhibitors. (J Bone Miner Res 2000;15:342–351)

# INTRODUCTION

Fracture repair is a reproducible cascade of cellular events that leads to bony union of the broken fragments. After a fracture, the space between the ends of the broken bones is filled with hematoma rich in pluripotential mesenchymal cells and cytokines.<sup>1, 2</sup> The tissue that forms within this space (callus) usually goes through a cascade of events that includes cartilaginous, ossification, and remodeling phases.<sup>3, 4</sup> The roles of growth factors,<sup>1, 2, 5-8</sup> eicosinoids,<sup>9</sup> and protooncogenes <sup>10</sup>in fracture healing have been studied. Despite these efforts, the regulatory mechanisms in fracture healing are not clearly understood.

Nitric oxide is a diatomic molecule and is classified as a free radical because of a readily available unpaired electron. NO is gaseous and very labile. It can rapidly diffuse through all membranes and organelles, both inside and outside the cell. In the presence of oxygen, it rapidly metabolizes to nitrates and nitrites.<sup>11</sup> NO is synthesized from the basic amino acid l-arginine, which in turn is synthesized as a product of the urea cycle and circulates in the blood at a concentration of ~100 μM. In the mammalian cell, the reaction of l-arginine to l-citrulline and NO is catalyzed by three isoforms of nitric oxide synthase (NOS), two of which are low-output constitutive (eNOS and bNOS) and one is high output inducible (iNOS). The volume of NO produced is regulated by calcium ion influx/effluxes in eNOS and bNOS.<sup>12, 13</sup> The production of iNOS usually is seen in response to an inflammatory stimulus, is regulated by iNOS gene expression,<sup>14</sup> and is calcium-independent.

NO produces its effect by many interrelated redox reactions with oxygen and transitional metal ions such as iron.<sup>15</sup> NO can bind to the heme group in enzymes, thereby leading to a change in the configuration of enzymes.<sup>16</sup> It is by this mechanism that NO activates guanylate cyclase, leading to formation of the second messenger cyclic guanosine monophosphate (cGMP), which in turn mediates many of the signaling functions of NO.<sup>16</sup> Examples of the indirect actions of NO are seen after its reaction with O<sub>2</sub> or superoxide anion (O<sub>2</sub><sup>-</sup>).<sup>17</sup> NO and O<sub>2</sub> form N<sub>2</sub>O<sub>3</sub>, which can modify thiol groups to form stable end products, which then can act as NO carriers. The reaction of NO and O<sub>2</sub><sup>-</sup> leads to the formation of peroxynitrite, which has cytotoxic properties and can nitrosylate tyrosine rings in proteins, leading to the formation of nitrotyrosine.<sup>17</sup>

NO plays important roles in many physiological functions, including the maintenance of blood pressure, in the central nervous system,<sup>12</sup> and in the host immune response.<sup>18</sup> Schaffer et al.<sup>19</sup> studied the modulatory role of NO in wound healing and showed that a systemic inhibition of NOS led to a decrease in wound breaking strength in a rat wound sponge healing model. We have studied the role of NO in tendon healing and have shown that NOS was induced during

tendon healing and that treatment with a NOS inhibitor impaired tendon healing.<sup>20</sup> We have also shown that treatment with a NOS inhibitor decreased mechanically induced new bone formation in a rat tibia model.<sup>21</sup>

With this background, we hypothesized that NO had a role in fracture healing. The aim of the first part of this study was to identify in a temporal fashion the presence or absence of NOSs in rat femoral fracture repair. The aim of the second part of the study was to evaluate the presence or absence of NOSs in healing fractures in humans. The third part of the study was designed to study rat fracture healing in NOS deficiency, and the last part studied the effect of NO supplementation on rat fracture repair.

## METHODS

### Materials

l-Nitroso-arginine methyl ester (l-NAME), d-nitrosoarginine methyl ester (d-NAME), reduced form of  $\beta$ -nicotinamide adenine dinucleotide phosphate (NADPH), calmodulin, valine, Dowex 50W anion-exchange resin, and tetrahydrobiopterin were obtained from Sigma Chemical Co. (St. Louis, MO, U.S.A.). Drugs for animal anesthesia and reagent-grade organic solvents were obtained from commercial suppliers. All antibodies were purchased from Transduction Laboratory (Lexington, KY, U.S.A.), and all primers for polymerase chain reaction (PCR) were synthesized by Life Technologies (Melbourne, VIC, Australia). The staining kit used with the iNOS antibody was purchased from Dako Corporation (Carpinteria, CA, U.S.A.).

### Animals and experimental designs

The Animals Ethics and Care Committee of the University of New South Wales approved all animal experiments. Male Sprague–Dawley rats (Biological Resources Centre, Sydney, NSW, Australia) with mean ( $\pm$ SD) weight of 318 g ( $\pm$ 2 g) were housed under a 12-h day/night light condition with 60% humidity at 21°C. Rats had either a closed or open midshaft right femoral fracture created. The right femur was fractured, and the left femur was used as an internal control. The anesthetic consisted of 300  $\mu$ g/kg ip of fentanyl (Hypnorm, Janssen; Buckinghamshire, U.K.) and 5 mg/kg midazolam. Postoperative pain relief was provided by preoperative injection of 2 ml of 0.5% marcaine (Astra Pharmaceuticals, North Ryde, NSW, Australia) around the fracture site, an intramuscular injection of 0.05 mg/kg of buprenorphine (Reckitt and Coleman, West Ryde, NSW, Australia) at the end of operation, and oral administration of buprenorphine (0.15 g/kg) via a jelly ad libitum for up to 3 days. All rats were euthanased by carbon dioxide inhalation.

*Closed-fracture model:* In 31 rats, a closed femoral fracture was created by three-point bending.<sup>22</sup> In brief, the right thigh of the anesthetized rat was placed between three points in the jaw of a modified forceps, and the jaws were rapidly closed to deliver a force that resulted in a reproducible fracture of the right femur. Rats were euthanased by carbon dioxide inhalation on days 4 ( $n = 7$ ), 7 ( $n = 6$ ), 10 ( $n = 4$ ), 15 ( $n = 7$ ), and 30 ( $n = 7$ ). Weight-matched rats ( $n = 6$ ) without fractures formed the control group. After each rat was euthanased, the fracture callus was dissected clean of surrounding tissues, snap-frozen in liquid nitrogen, and stored at  $-80^{\circ}\text{C}$  until protein and mRNA studies were carried out. Samples from day 10 were processed for immunohistochemistry.

*Open-fracture model:* With an aseptic surgical technique, a 2-cm incision was made on the lateral aspect of the right thigh. Fascia, muscle, and periosteum were sharply incised, and the subperiosteal muscles were dissected. A controlled midshaft femoral fracture was made with a gigli saw. The osteotomy was then fixed with a 1.6-mm-diameter stainless-steel Kirshner wire (K-wire), which was first passed retrograde into the proximal fragment and then into the medullary canal of the distal fragment. Rats were fed either an inhibitor of NOS, d-NAME (1 mg/ml ad libitum in drinking water;  $n = 20$ ), or its inactive enantiomer, d-NAME (same dose;  $n = 20$ ) from 2 days before surgery until the end of experiment, on day 24.

To determine whether local administration of NO could enhance fracture healing, transverse midshaft femoral fractures were created in four groups of rats. The two treatment groups either received local implantation of a NO donor (a NONOate derivative of carboxybutyl chitin or chitosan, CBC-NO;  $n = 11$ ) or were fed d-NAME, an NO inhibitor ( $n = 13$ ). The control groups consisted of local administration of the vehicle chitosan (CBC;  $n = 11$ ) alone or oral administration of d-NAME ( $n = 13$ ). Chitosan is a nonacetylated or partially deacetylated chitin (a linear homopolymer of  $\beta$ -(1–4)-linked *N*-acetylglucosamine). It is biocompatible and has been used for local delivery of drugs.<sup>23, 24</sup> Two hundred milligrams of CBC-NO that releases 250 nmol NO per 5 mg of CBC-NO over 185 minutes was used to deliver NO locally to the fracture site. CBC and CBC-NO were obtained from Daniel Smith of University of Akron (Akron, OH, U.S.A.). At the end of the experiment (day 17 after fracture), both hindlimbs were disarticulated at the hip and stored at  $-80^{\circ}\text{C}$  until dual-energy X-ray absorptiometry (DEXA) scan, callus morphometry, and biomechanical analyses were performed.

## Human fracture callus

Fracture callus was collected from six patients undergoing open reduction and internal fixation of a fracture. Fresh samples were snap-frozen in liquid nitrogen and stored at  $-80^{\circ}\text{C}$  until

immunoperoxidase staining and RNA extraction was carried out. Procurement of tissue at surgery was approved by the Human Ethics Committee of the South Eastern Sydney Area Health Service.

## NOS activity assay

Fracture callus was crushed and ground with a mortar and pestle in liquid nitrogen, and the sample was divided into two. Each portion was mixed with a homogenization buffer that consisted of 50 mM Tris-HCl, 0.1 mM EDTA, 0.1 mM ethylene glycol-bis( $\beta$ -amino ethyl ether)-*N,N,N',N'*-tetraacetic acid (EGTA), and 12 mM 2-mercaptoethanol (pH 7.4) with a cocktail of protease inhibitors (2  $\mu$ g/ml leupeptin, 5  $\mu$ g/ml pepstatin A, 500  $\mu$ g/ml AEBSF [4-(2-aminoethyl)benzenesulfonyl fluoride] and 1  $\mu$ g/ml E-64 [trans-epoxysuccinyl-L-leucylamido-(4-guanidion)butane]. NOS activity was estimated by using a conversion assay of [ $^3$ H]l-arginine to [ $^3$ H]l-citrulline.<sup>25</sup> In short, 30  $\mu$ l of tissue homogenate was incubated in the presence of 10  $\mu$ M [ $^3$ H]l-arginine (5 kBq/tube), 1 mM NADPH, 5  $\mu$ M tetrahydrobiopterin, 50 mM valine, 2 mM calcium, and 30 nM calmodulin for 30 minutes at 37°C. The reaction was stopped by adding 500  $\mu$ l of cold HEPES buffer (pH 5.5) that contained 2 mM EGTA and 2 mM EDTA. This reaction mixture was then centrifuged through a Dowex (Na<sup>+</sup> form 50W), and the eluant was measured for [ $^3$ H]l-citrulline activity in a  $\beta$ -counter (Minaxi Tri-Carb 4000S, United Technologies, Packard; Downers Grove, IL, U.S.A.). Parallel experiments were performed in the presence of calcium chelator (EGTA, 5 mM) and in the presence of the NOS inhibitor *N*<sup>G</sup>-monomethyl-l-arginine (l-NMMA; 3 mM). These parallel experiments were done to determine the concentration of calcium-dependent NOS and to determine the extent of formation of [ $^3$ H]l-citrulline that was independent of any NOS activity, respectively. Values of [ $^3$ H]l-citrulline detected within the blanks were subtracted from all values, and the activity of calcium-dependent and calcium-independent NOS was calculated. Protein concentration of the homogenates was estimated by using Commassie Plus Reagent (Pierce; Rockford, IL, U.S.A.) according to the manufacturer's instructions.

## Immunoprecipitation and Western blot for NOS

Five hundred microliters of tissue homogenate was precleaned with 100  $\mu$ l of protein A-agarose (Bio-Rad, Los Angeles, CA, U.S.A.) for 1 hour at 4°C. The precleaned homogenate was incubated with 0.5  $\mu$ g of monoclonal anti-iNOS antibody (Transduction Laboratories) at 4°C overnight and then with protein A-agarose for 1 h at 4°C, washed three times, resuspended in Laemmli<sup>26</sup> sample buffer (125 mM Tris-HCl, pH 6.8, 10% [v/v] glycerol, 4% [v/v] sodium dodecyl sulfate [SDS]), boiled for 5 minutes, and then pelleted. Supernatants containing 20  $\mu$ g

of protein were loaded into each well of a 7.5% (v/v) SDS–polyacrylamide gel electrophoresis (SDS-PAGE) gel. Fractionated proteins were transferred from the gel to a polyvinylidene difluoride (PVDF) membrane and blocked with 5% (w/v) skimmed milk in 0.1% (v/v) TTBS (0.1% Tween-20 in 20 mM Tris and 137 mM NaCl, pH 7.6) buffer overnight at 4°C. The blocking solution was poured off, and the membrane was washed with two changes of TTBS under agitation. The membrane was then incubated in a plastic bag with the iNOS monoclonal antibody (1:2000 in 1% bovine serum albumin [BSA] in TTBS) for 1 h at room temperature. The membrane was then washed three times, 10 minutes each with TTBS. The secondary antibody used for incubating the membrane for the next 1 h was an anti-sheep immunoglobulin G (Selenius Lab; Melbourne, VIC, Australia) (1:2000 dilution) conjugated to horseradish peroxidase (HRP) in TTBS buffer containing 1% (w/v) BSA. The membrane was washed twice with TTBS and twice with Tris-buffered saline (TBS) for 10 minutes each time, and immunoreactive bands were detected by using an enhanced chemiluminescence reagent (Pierce; Rockford, IL, U.S.A.). Macrophage lysate was used as a positive control for iNOS.

## Immunohistochemistry of fracture callus

Rat femoral shaft fracture callus was fixed in 4% (v/v) formaldehyde for 12 h at 4°C, decalcified in 0.1% (w/v) EDTA at room temperature for 10 days, sectioned in the sagittal plane, and processed by serial dehydration in acetone and then ethyl alcohol. Samples were embedded in paraffin, and 7- $\mu$ m-thick sections were cut. The sections were placed in an antigen-retrieval solution (Dako) and placed in a microwave for 10 s to unfold antigenic epitopes. Endogenous peroxidase was blocked with 3% hydrogen peroxide for 10 minutes, and background proteins were blocked with 2% (w/v) skimmed milk for 15 minutes. Thereafter, a monoclonal antibody for murine iNOS (Transduction Lab) was incubated with 200  $\mu$ g/ml phosphate-buffered saline (PBS) at room temperature for 60 minutes. The reaction was visualized with streptavidin–HRP immuno-histochemistry by using a large-volume peroxidase kit (Dako) according to the manufacturer's instructions. Diaminobenzidine was used as chromogen, and hematoxylin as a nuclear counterstain. Control sections in which the primary antibody was omitted were used in each run to control for nonspecific binding of the secondary antibody. The sections were mounted in 80% (v/v) glycerol in PBS and studied under a Leica microscope (Leica Mikroskopie and Systeme, Wetzlar, Germany).

## Reverse-transcription PCR for NOS isoforms

Rat right femoral cortex without the marrow and periosteum from uninjured rats and external fracture callus from the right femur of injured rats were ground to a fine powder by using a

mortar and pestle under liquid nitrogen in RNAase-free conditions. Total RNA was extracted by using Trizol Reagent (Life Technologies) according to the manufacturer's instructions. Complementary DNA was synthesized from total RNA by reverse transcription. PCR reactions were carried out by using Taq polymerase (Promega, Madison, WI, U.S.A.) with primers designed for murine NOS isoforms. Primer sequences (5' to 3') corresponding to their location on respective genes were as follows: for iNOS, 1948–2170; [27](#) for eNOS, 2169–2721; and for bNOS, 3726–4005.[27](#) For human NOS isoforms,[28](#) the corresponding primer sequences were as follows: for iNOS, 1425–1924; for eNOS, 1050–1535; and for bNOS, 4207–4672. The housekeeping gene,  $\beta$ -actin (405–1048), was used as an internal control for determination of the efficiency of RNA extraction, reverse transcription, and PCR steps. Initial denaturing was done at 94°C for 4 minutes, and the thermal cycling was carried out at 94°C for 50 s, 57°C for 45 s, and 72°C for 90 s for 30 cycles. After the final cycle, the products were further extended at 72°C for 5 minutes and then held at 4°C until separation. PCR products were separated on 1.5% (w/v) agarose gel with 0.1% (w/v) ethidium bromide in TAE buffer (40 mM Tris-acetate, 1 mM EDTA) by using pUC19 as DNA markers. The gel was visualized and photographed with UV back-illumination.

## DEXA scan and callus morphometry

Bone mineral density was measured on thawed specimens with DEXA using hand-regional high-resolution mode on a Lunar Expert XL (Lunar Corporation, Madison, WI, U.S.A.). The line spacing was 0.254, and point resolution was 0.890 mm. Point types were marked out to delineate the bone and exclude soft tissue and artefact created by the K-wire. The regions of interest included the entire right femur without the K-wire, an 8 mm  $\times$  7 mm rectangle centered on the fracture site, and the entire left femur as internal control. Bone mineral density values are reported in grams per square centimeter.

After the DEXA scan, each femur was dissected clean from the surrounding tissues, and the diameter of the callus was measured in two planes, in the region where the callus was thickest, by using a vernier caliper (Mitutoyo, Kawasaki, Japan). Cross-sectional areas were calculated and represented as a percentage of the unoperated left side. Both the fractured femur and intact femur were stored in PBS at  $-20^{\circ}\text{C}$  until biomechanical analysis.

## Biomechanical analysis

After removing the K-wire from a distal portal, femurs were subjected to three-point bending to failure on a AG-50KNE material testing machine (Shimadzu, Kyoto, Japan) with a jig span of 18 mm at a displacement rate of 5 mm/minute. Load displacement data was acquired with a 50-N

load cell for the rate of 200/s. Load-displacement curves were plotted, and failure load, stiffness, and energy were calculated for each sample.<sup>29</sup> The unoperated left side was used as internal control.

## Statistical analysis

All data are reported as means  $\pm$  SEM. Differences among the groups were assessed by using unpaired two-tailed Student's *t*-tests to compare groups. The level of statistical significance was set at  $p < 0.05$ .

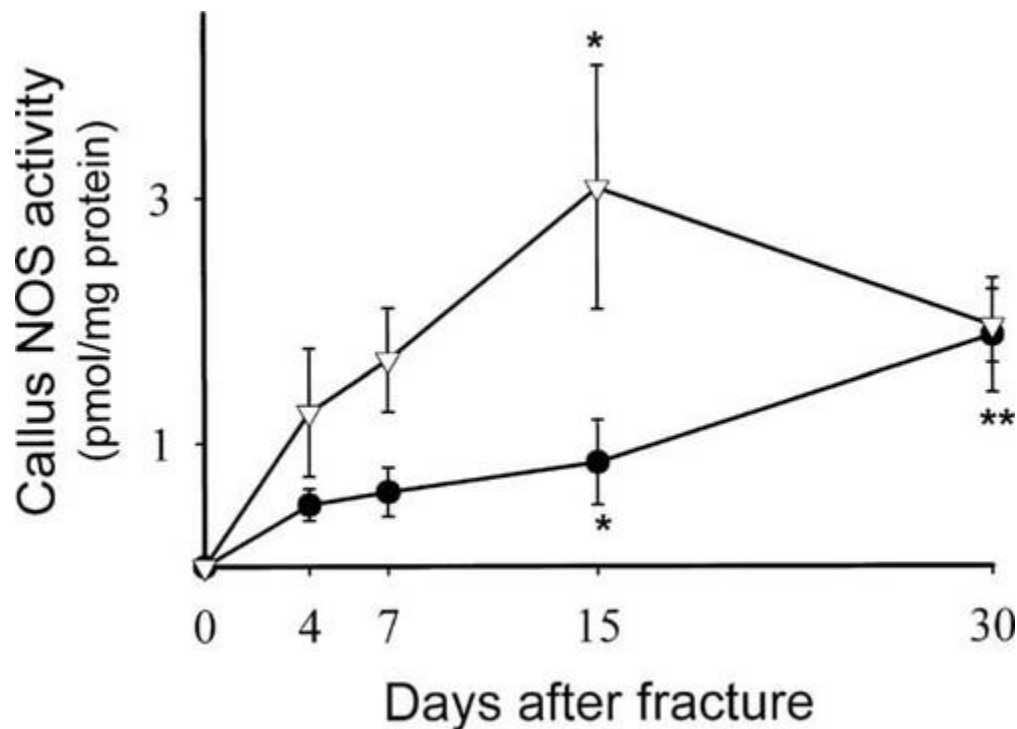


**Figure Fig. 1.**

[Open in figure viewerPowerPoint](#)

Temporal expression of NOS in a rat closed femoral fracture model. Using a conversion assay of [<sup>3</sup>H]arginine to [<sup>3</sup>H]-citrulline, there was no detectable NOS activity in intact femurs.  $\bullet$ , calcium-dependent NOS activity;  $\nabla$ , calcium-independent NOS activity. Controls consisted of right femurs of weight-matched rats without a fracture. Values are means  $\pm$  SEM of two independent determinations performed in duplicate for each sample in all experimental groups ( $n = 6$  rats for each time point). \* $p < 0.05$  and \*\* $p < 0.01$  compared with controls by using unpaired two-way Student's *t*-tests.

## RESULTS

### Temporal expression of NO in rat fracture healing

No calcium-independent NOS activity was observed in the right femurs of uninjured rats. In the right healing femurs, calcium-independent NOS activity was detected on days 4, 7, 15, and 30 after fracture; the maximum was on day 15 ( $p \leq 0.05$ ) (Fig. 1). No calcium-dependent NOS activity was observed in the rat right femurs before fracture. On day 4 after fracture, the average level of calcium-dependent NOS was 30% of the average level of calcium-independent NOS on the same day. The calcium-dependent NOS in healing rat femurs increased four folds from day 4 to day 30 after fracture (Fig. 1).

## Inducible NOS protein detection

The presence or absence of protein for iNOS was detected by immunoprecipitation followed by SDS-PAGE. Mouse macrophage lysate was used as a positive control (130 kDa).

Immunoprecipitation of rat femur homogenates with a specific monoclonal antibody directed against iNOS showed no immunoreactivity in unfractured bone. Immunoreactive bands were detected in fracture callus homogenates at days 4, 7, 15, and 30 after rat femoral shaft fracture (Fig. 2). The anti-iNOS immunoblots of fracture callus revealed two bands, migrating on the SDS-PAGE, with apparent molecular masses of 136 kDa and 96 kDa.

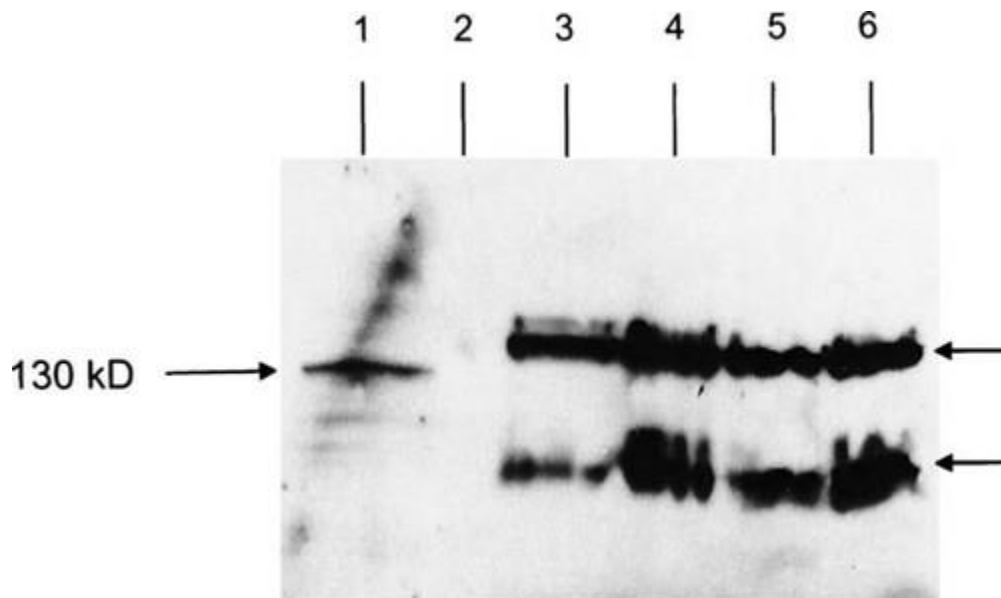


**Figure Fig. 2.**

[Open in figure viewerPowerPoint](#)

Immunoprecipitation of rat fracture callus using an anti-mouse iNOS monoclonal antibody. (Lane 1) iNOS-positive control (130 kDa), stimulated mouse macrophage lysate. (Lane 2) Homogenate of unfractured rat femur bone. (Lanes 3, 4, 5, and 6) Femurs at days 4, 7, 15, and 30 after fracture, respectively. Notice two bands corresponding to 136 kDa and 95 kDa in lanes 3–6.

## Immunolocalization of iNOS

In the absence of the primary antibody, there was no brown immunostaining in the callus tissue section (Fig. 3C). Elongated fibroblast-like cells in the external day-10-callus did not show any brown immunostain. Cells at the junction of fibrous tissue and the cartilage front showed immunostaining for the iNOS protein (Fig. 3A). Immunostaining for iNOS protein was also seen in the large round chondroid-type cells extending up to the junction of the cartilage and the new bone (Fig. 3B).

## NOS mRNA in rat fracture healing

NOS gene expression was evaluated in the same model using reverse-transcription PCR (RT-PCR) of mRNA extracted from fracture calluses with primers specific for iNOS, eNOS, and bNOS genes.  $\beta$ -Actin primers were used as internal controls.  $\beta$ -Actin was detected in mRNA of unfractured femoral bone cortex and fracture callus from all time points. No iNOS, eNOS, or bNOS mRNA was detected in the RNA extracted from the cortex of unfractured rat femurs; however, mRNA for iNOS were detected in fractured rat femurs on days 4, 7, and 15 after fracture, and mRNA for eNOS and bNOS were detected on days 7 and 15 after fracture in the RNA extracted from external callus (Fig. 4).

## NOS isoforms in human fracture healing

mRNA extracted from human fracture callus from separate patients were subjected to RT-PCR. Internal control  $\beta$ -actin gene expression was detected for all samples. The iNOS and eNOS mRNA were detected in all samples of human fracture callus; bNOS mRNA was found in a sample collected from a patient with a 90-day-old fracture and not in samples of 3- to 6-day-old fractures (Fig. 5).

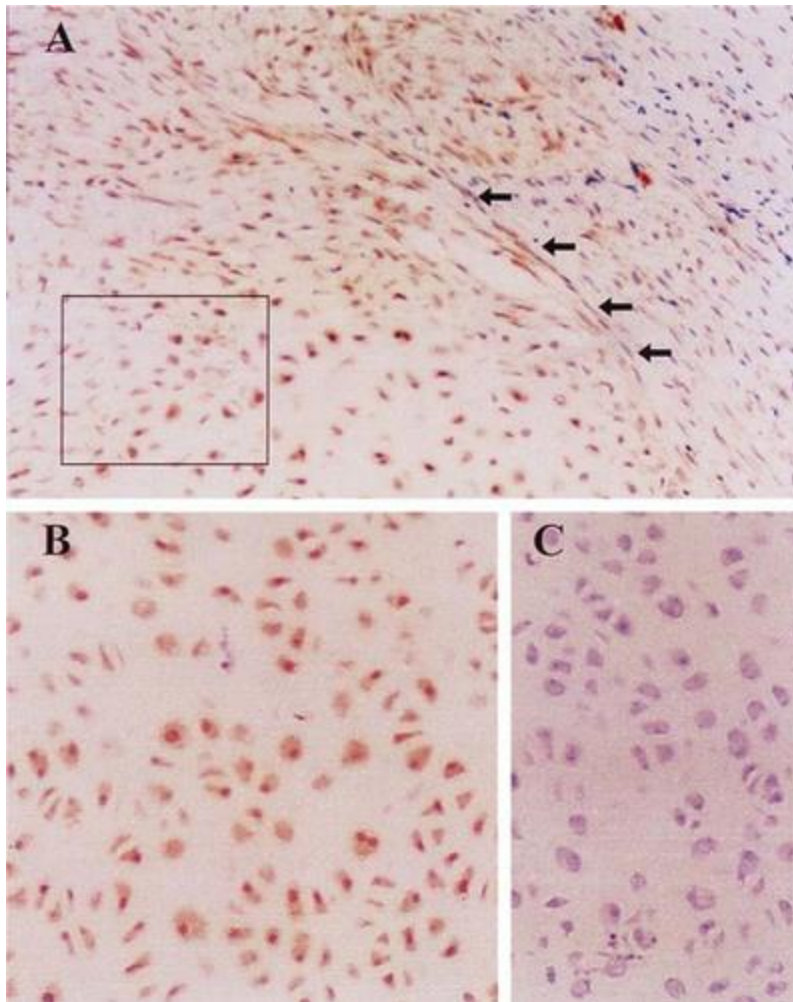


**Figure Fig. 3.**

[Open in figure viewer](#)**PowerPoint**

Immunolocalization of iNOS in rat femur 10-day-old fracture callus. (A) Immunoreactivity (brown discoloration) is noted in cells at the junction of fibroblast-like cells and chondroid cells (magnification = 100×). (B) Immunoreactivity of chondrocyte-like cells in the region of enchondral ossification (magnification = 400×). (C) Negative control; same section as (B) but without primary antibody.

## Impaired fracture healing on NOS inhibition

Rats were fed either the NOS inhibitor l-NAME or its inactive enantiomer d-NAME in a dose of 1 mg/ml of water ad libitum starting 2 days before surgery (to ensure preinjury NOS inhibition) and throughout the experimental period of 24 days. All rats recovered from surgery uneventfully. Rats in both group gained an average of 30% of their original body weight during this period (Table 1).

*Callus morphology:* Oral administration of l-NAME did not alter the cross-sectional area of the uninjured femurs. However, a 20% ( $p \leq 0.001$ ) decrease in cross-sectional area of the healing fracture callus was observed in rats fed l-NAME (Fig. 6A).

*Mineral content:* There was no difference in bone mineral content of the unoperated femur in rats fed l-NAME and those fed d-NAME. With inhibition of NO synthesis (rats fed l-NAME), however, a 20% decrease was observed in the average mineral density of the callus compared with the control group (Table 2).

*Biomechanical analysis:* In a three-point bending test, all femurs displayed a load-displacement curve typical for a long bone: An initial nonlinear response was followed by an upward sloping linear component, then a failure response at the point of break (Fig. 6B). There was a 45% ( $p < 0.05$ ) decrease in peak failure load, a 55% decrease in stiffness and 48% decrease in energy required to break the healing rat right femur on day 24 in the NOS-inhibited group compared with the control group (Table 2). All healing femoral fractures failed at the fracture site on three-point bending in both groups. The left unoperated femur always failed with a transverse break at the midshaft. There was no alteration in the mechanical properties of the unfractured left femur with NOS inhibition (in rats fed l-NAME) or without (in rats fed d-NAME).

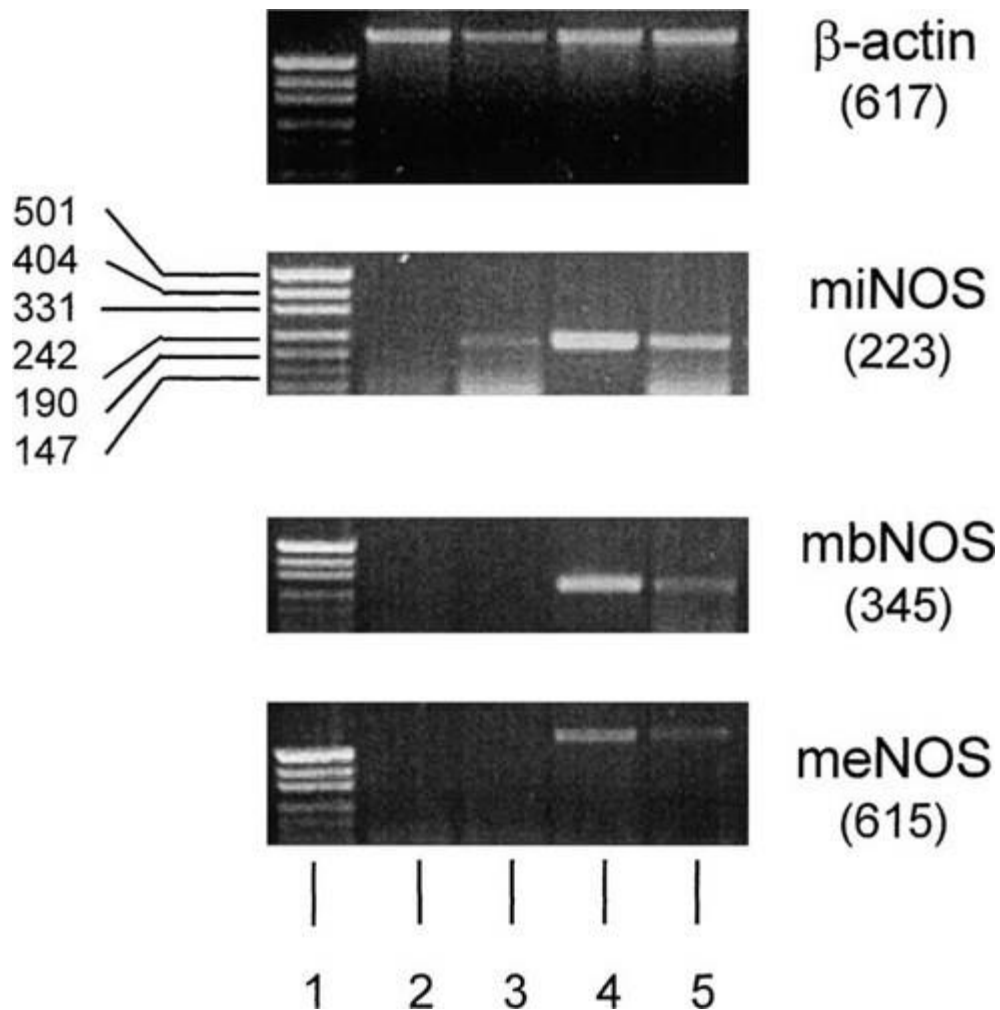


**Figure Fig. 4.**

[Open in figure viewer](#)**PowerPoint**

NOS gene expression. Transcripts of iNOS, bNOS and eNOS in rat femurs at days 4, 7, and 15 after fracture by RT-PCR using rat-specific oligonucleotides (m = murine) iNOS, bNOS, and eNOS.  $\beta$ -Actin was used as an internal control. Lane 1, pUC19 as DNA marker. Lane 2, unfractured rat right femoral cortex alone. Lane 3, right femur at day 4 after fracture. Lane 4, right femur at day 7 after fracture. Lane 5, right femur at day 15 after fracture. Numbers in parentheses indicate the size of PCR products (in bp).

## Reversal of impaired fracture healing by an NO donor

In the NO donor experiment, at day 17 after fracture, the NO supplemented (CBC-NO) group had a 20% increase in cross-sectional area of fracture callus compared with the chitosan control (CBC) group and a 30% ( $p \leq 0.01$ ) increase in cross-sectional area compared with the NOS inhibition (l-NAME) group (Fig. 7).

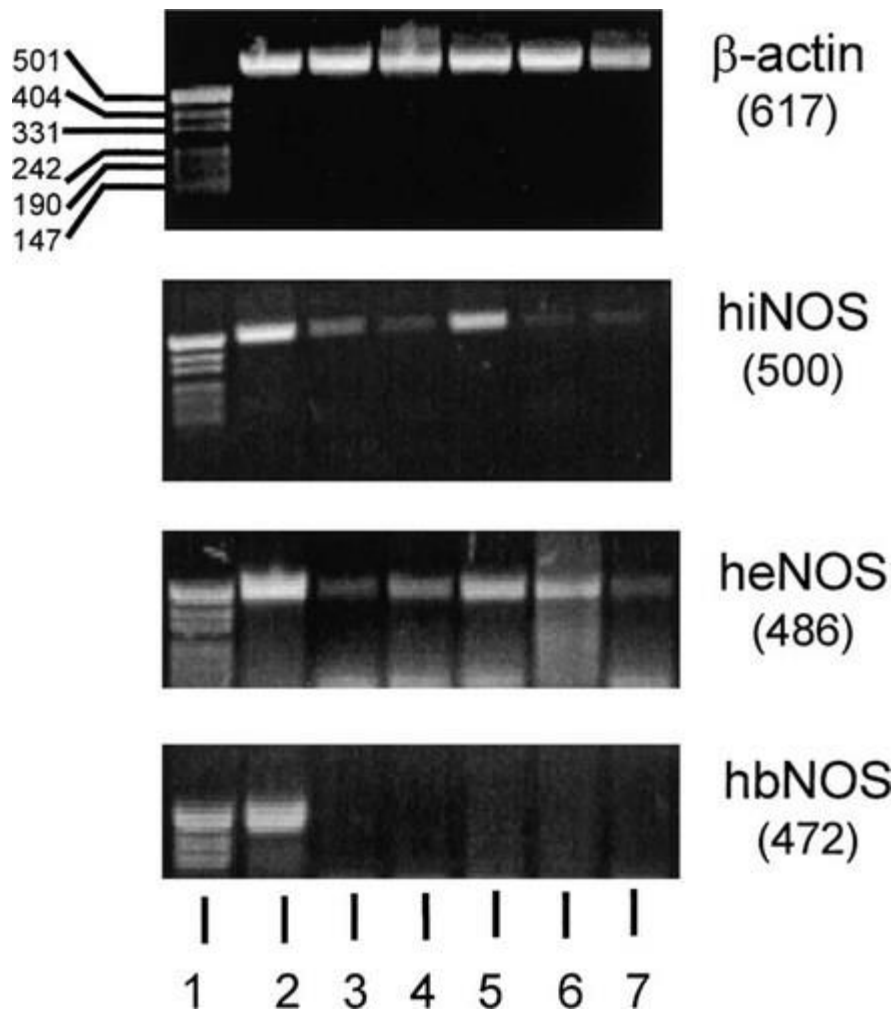


**Figure Fig. 5.**

[Open in figure viewerPowerPoint](#)

RT-PCR for the transcripts of NOS isoforms in samples of human (h) fracture callus procured from patients undergoing open reduction and internal fixation of a fracture. Lane 1, pUC19 as DNA marker. Lane 2, 90-day-old callus. Lanes 3–6: 3- to 5-day-old fracture callus from different patients.

**Table Table 1..** Body Weights of Rats with NOS Inhibition

	<i>d-NAME</i>	<i>l-NAME</i>	<i>p value</i>
Weight (g)			

	<i>d-NAME</i>	<i>l-NAME</i>	<i>p value</i>
Initial	319 ± 2	318 ± 2	0.60
Final	419 ± 6	419 ± 6	1.00

- Initial, 2 days before surgery (i.e., the day the drugs were started); final, at day 24 (when rats were killed). Values are mean ± SD.

## DISCUSSION

In this report, we show for the first time a temporal expression of all three isoforms of NOS (iNOS, eNOS, and bNOS) during rat femoral fracture healing. We found no evidence of NOS activity in unfractured cortical bone. iNOS and the constitutive NOSs (eNOS and bNOS) were expressed at different stages of fracture healing. iNOS was induced on day 4 and peaked on day 15 of fracture healing, whereas eNOS and bNOS were expressed in significant amounts on day 15 of fracture healing, stages associated with remodeling of fracture callus. These findings of differential expression of NOS isoforms in a temporal manner during fracture healing are consistent with our previous finding of a bimodal expression of serum nitrate (a stable end product of NO) in rat fracture healing.<sup>30</sup> We observed an elevated serum nitrate concentration on day 7 and a second peak at day 21 in a closed femoral fracture model. The initial peak may have corresponded to early iNOS expression and the second peak to increased eNOS and/or bNOS expression. In the experiments reported here, we were unable to separate the contributions of eNOS and bNOS to the gradual increase in constitutive NOS seen in later stages of fracture healing. Furthermore, because our experiments ended on day 30, we were unable to determine at what point NOS returned to the baseline levels (if at all).

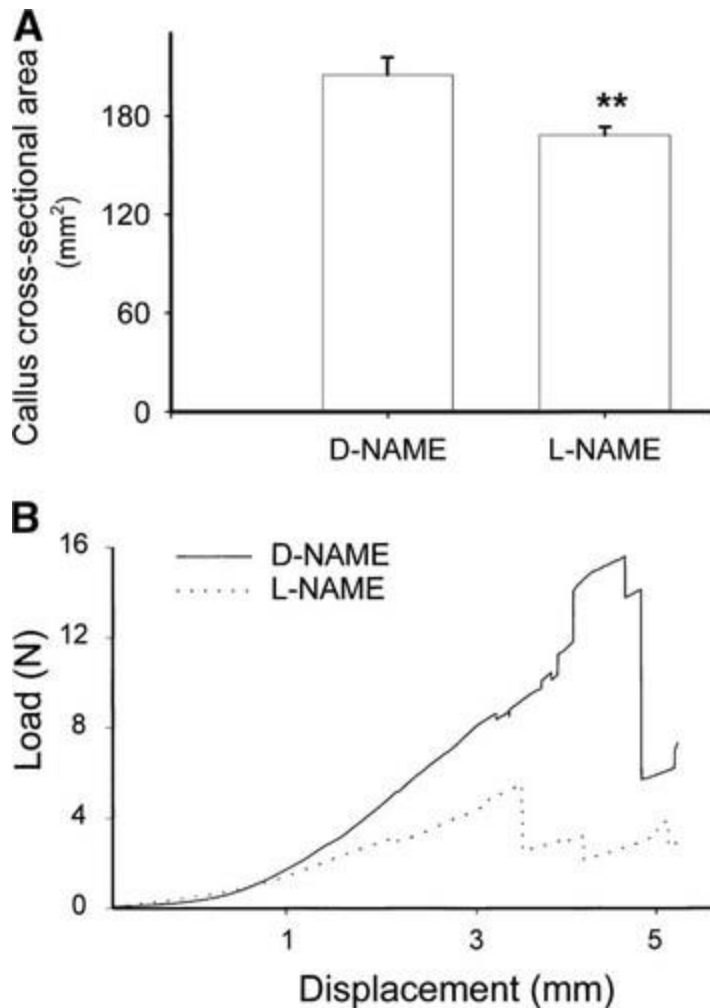


**Figure Fig. 6.**

[Open in figure viewer](#)**PowerPoint**

Effects of a NOS inhibitor on rat femur fracture healing. Rats were fed either the NOS inhibitor l-NAME or its inactive enantiomer, d-NAME (1 mg/ml of water ad libitum) starting 2 days before surgery, when a midshaft fracture was created and fixed internally with K-wire (open-fracture model). (A) Cross-sectional area at day 24.  $**p \leq 0.01$  compared with the control (d-NAME) group, using unpaired two-tailed Student's *t*-tests ( $n = 18$  femurs for each group). Values are means  $\pm$  SE. (B) Mean load-displacement curves on three-point bending to failure for callus in rats fed the NOS inhibitor (l-NAME;  $n = 16$ ) versus control rats (d-NAME;  $n = 16$ ) on day 24 after fracture. There was no difference for load-displacement curves of the left side unoperated internal control femurs (not shown).

We identified iNOS at a transcriptional, translational, and biochemically active level in a closed rat femoral fracture model. The anti-iNOS immunoblots of fracture callus revealed two bands, migrating on the SDS-PAGE, with apparent molecular masses of 136 kDa and 96 kDa. Similar

doublets of varying molecular masses for iNOS have been reported for murine macrophages<sup>31, 32</sup> and murine hepatocytes.<sup>33</sup>

**Table Table 2..** Effect of NOS Inhibition on Rat Healing Fracture

	<i>d-NAME</i>	<i>l-NAME</i>	<i>p value</i>
Callus mineral density (g/cm <sup>2</sup> )	160 (16)	130 (6)	0.10
Cross-sectional area* (mm <sup>2</sup> )	353.1 (16.7)	287.7 (9.5)	0.001
Failure load (Newtons)	9.4 (1.9)	5.1 (1.2)	0.05
Stiffness (N/mm)	2.2 (0.4)	1.2 (0.2)	0.02
Energy (N · mm)	25.4 (7.2)	13.3 (3.5)	0.13

- \*Results are expressed as percent change compared with paired unfractured left side. *p* values were estimated for unpaired Student's *t*-tests applied to compare groups.

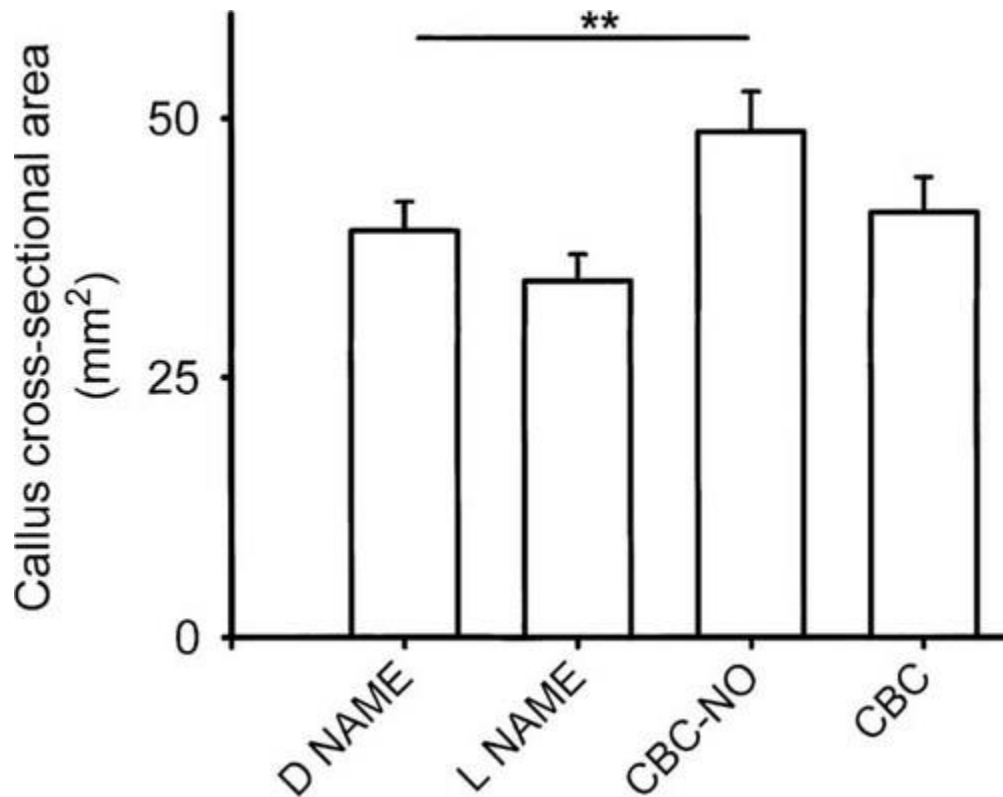


**Figure Fig. 7.**

[Open in figure viewerPowerPoint](#)

Effect of NO supplementation on fracture healing in rats. In an open-fracture model, a CBC-NO that releases 250 nmol NO per 5 mg over 185 minutes was used to deliver NO locally in a dose of 200 mg to the fracture site ( $n = 11$  rats). The vehicle chitosan (CBC) alone was delivered locally at the time of the operation as a control ( $n = 11$ ). NOS was inhibited by feeding a group of rats l-NAME (1 mg/ml ad libitum starting 2 days before surgery;  $n = 13$ ). The control group was fed the inactive enantiomer d-NAME group (same dose;  $n = 13$ ). A statistically significant 30% increase in callus cross-sectional area was seen in the group that received NO donor carboxybutyl chitosan NONOate compared with the NO-deficient group (l-NAME fed rats) using an unpaired Student's *t*-test.  $**p < 0.01$ .

Evaluation of human fracture callus mRNA for isoforms of NOS by RT-PCR revealed the presence of iNOS mRNA and eNOS mRNA in all samples. The mRNA for bNOS was observed only in a 90-day-old callus sample. Human fracture callus contain macrophage-like cells, which stain positive with antibodies for Mac387 and CD68 antigens, at all stages of fracture repair.<sup>34</sup> Because human inflammatory macrophages are known to produce iNOS,<sup>18</sup> the presence of iNOS in human fracture healing may be related to the presence of macrophages during this process. These results provide preliminary evidence for the presence of NOS in human fracture healing.

The present studies are the first time that isoforms of NOS have been detected in fracture callus, and the question of which cells make NOS remains incompletely answered. Fracture healing is a cascade of cellular events that involve a range of cellular phenotypes, including but not limited to platelets, wound macrophages, wound fibroblasts, chondrocytes, osteoblasts, and osteoclasts. All these cell types express iNOS.<sup>27, 35-39</sup> Schaffer et al.<sup>37</sup> have shown by in situ hybridization that iNOS was expressed by wound macrophages and wound fibroblasts within subcutaneously implanted sponges on day 10 after surgical incision and implantation in a rat wound sponge healing model. Using immunohistological techniques, Yamanaka et al.<sup>36</sup> showed expression of iNOS by accumulated macrophages in a surgically induced rat brain injury model on day 3. Our immunohistological studies at day 10 of fracture healing in rats showed iNOS expression in fibroblasts and chondrocytes in the callus (Fig. 3).

There are no studies addressing the cellular localization of eNOS or bNOS in healing models. However, eNOS expression has been evaluated in other inflammatory situations. Steudel et al.<sup>40</sup> showed by immunohistology in a hyperoxia-induced pulmonary hypertension model in adult rats that the expression of eNOS was significantly increased in both the endothelial cells and macrophage-like cells by day 28 of hyperoxia. Fox et al.<sup>39</sup> demonstrated immunohistologically that eNOS was constitutively expressed by cells of osteoblastic lineage in the tibia and in hypertrophic chondrocytes of the vertebral growth plates of adult rats and that chondrocytes and osteoclast-like cells were strongly positive for eNOS in vertebrae and ribs of 3-day-old neonatal rats.

Data with respect to the expression of bNOS in inflammatory cells is limited. Ormerod et al.<sup>41</sup> studied the inflammatory skin condition psoriasis. They observed a pattern of spatial expression of NOS isoforms depending on the area of tissue involved by the disease in their study of psoriatic skin, uninvolved skin of psoriatic patients, and normal skin by using immunohistological techniques. eNOS was constitutively expressed in normal skin, whereas iNOS staining was strongest in severe lesions. bNOS normally associated with keratinocytes in the granular layers was diffusely present throughout all layers of the epidermis in the uninvolved skin of psoriatic patients.<sup>41</sup> bNOS was not found by Fox et al.,<sup>39</sup> who used immunohistology in adult rat tibiae, neonatal rat bones, and adult human bone trephines and vertebrae of 16- to 32-week-old human fetuses. Additional experiments will be necessary to determine which cell types express each of the isoforms of NOS during the course of fracture healing.

In the present report, we show that NO is important in fracture healing. The magnitude of the healing response after fracture of rat femur was reduced by systemic administration of a NOS inhibitor (l-NAME). Inhibition of NOS led to a mechanically inferior callus that exhibited

reduced failure load, stiffness, and energy to failure in the l-NAME fed rats. The hypothesis that NO is important for healing of wounded tissues in general is supported by data from a range of animal models. Schaffer et al.<sup>19</sup> showed in a rat wound sponge healing model that a continuous intraperitoneal infusion of *S*-methyl isothiuronium (MITU, a competitive inhibitor of NO synthase) significantly decreased wound-breaking strength at day 10 after wounding. Murrell et al.<sup>20</sup> showed in a rat Achilles tendon healing model that administration of l-NAME led to a 30% decrease in cross-sectional area and 25% decrease in load to failure on tensile testing at day 7 after surgical transection of the tendon. Konturek et al.<sup>42</sup> found a significant decrease in healing rate of acetic acid-induced gastric ulcers in rats fed inhibitors of NOS, *N*<sup>G</sup>-nitro-l-arginine (l-NNA) or l-NMMA.

One of our concerns while evaluating the results of NO synthase inhibition in fracture healing is that it may be difficult to separate the systemic effect of NO synthesis inhibition from its specific effects on fracture healing. An independent role for NO in fracture healing was supported by the observation that a decrease in callus size and biomechanical parameters in the NOS-inhibited group was not accompanied by a similar decline in body weight.

We also found that addition of NO can reverse the impaired healing caused by NOS inhibition. There was a 30% increase in callus size with local NO supplementation compared with the NOS-inhibited state in our nitric oxide donor studies (Fig. 7). Addition of NO has also enhanced healing of other tissues in animal models. Shabani et al.<sup>43</sup> found a 25% enhancement of the healing rate in a rat full-thickness skin wound–healing model in a group that received a polyethyleneimine polymer delivering NO. Yamasaki et al.<sup>44</sup> found a 30% decrease in wound closure rate of excisional wounds in iNOS knock-out mice derived from the original C57BL/6J × 129 lines compared with the wild-type mice and that this delay in healing was fully reversed by a single topical application of an adenoviral vector containing the human iNOS cDNA.

The present studies do not address the likely mechanism(s) by which NOS may regulate and enhance fracture healing.

In summary, the studies outlined in this report suggest that NOS is induced during fracture healing in rats and in humans. Systemic inhibition of these enzymes reduced the magnitude of the fracture-healing response, whereas supplementation of NO to fracture healing augmented the process in rats. These results have potential clinical significance in that NO might enhance fracture healing, especially in situations in which fracture healing is impaired (e.g., malnutrition and diabetes). Similarly, the reverse may also hold true; that is, selective local inhibition of NO

synthesis may inhibit unwanted new bone formation in clinical situations such as myositis ossificans and postoperative heterotopic ossification in patients with ankylosing spondylitis.

## Acknowledgements

The authors thank Z. Szomor, A.Q. Wei, and J.H. Lin for help with the animal work; J. Jensen for help with the DEXA scans; M. Swain (University of Sydney) for providing his facility for biomechanical analyses; and N. Arora for technical support.

The Orthopaedic Research Institute is supported by the South Eastern Sydney Area Health Service and the Health Care of Australia Pty Ltd.

## References

## Notes :

- Initial, 2 days before surgery (i.e., the day the drugs were started); final, at day 24 (when rats were killed). Values are mean  $\pm$  SD.
- \*Results are expressed as percent change compared with paired unfractured left side. *p* values were estimated for unpaired Student's *t*-tests applied to compare groups.